Solid-State ^{13}C NMR Analyses of the Orthorhombic-to-Hexagonal Phase Transition for Constrained Ultradrawn Polyethylene Fibers

Kazuhiro Kuwabara and Fumitaka Horii*

Institute for Chemical Research, Kyoto University, Uji, Kyoto 611-0011, Japan

Received May 4, 1999; Revised Manuscript Received June 24, 1999

ABSTRACT: The orthorhombic-to-hexagonal phase transition for constrained ultradrawn polyethylene fibers has been investigated by solid-state ^{13}C NMR spectroscopy. In the CP/MAS ^{13}C NMR spectra, the resonance line assignable to CH_2 carbons in the hexagonal phase appears above 147 °C upfield compared to the line in the orthorhombic phase. The calculation of the ^{13}C chemical shift has revealed that 7% gauche defects are included in the hexagonal phase. In the CP/DD ^{13}C NMR spectra measured by setting the orientation axis perpendicular to the static magnetic field, two resonance lines assignable to σ_{11} and σ_{22} for the CH_2 carbons that appear in the orthorhombic phase merge to a single resonance line at an upfield position compared to the average of σ_{11} and σ_{22} in the hexagonal phase. On the other hand, when the orientation axis is set parallel to the static magnetic field, no remarkable change is observed in the hexagonal phase for the resonance line appearing at σ_{33}. These experimental results indicate that gauche defects such as kinks should be introduced at random along each molecular chain, and independent jump rotations occur around the molecular chain axis for the sequences between the gauche defects in the hexagonal phase. It has been also found that the 180° jump rotation around the molecular chain axis is induced in the orthorhombic phase at temperatures near the orthorhombic-to-hexagonal phase transition.

Introduction

It is well-known that the orthorhombic-to-hexagonal phase transition occurs in polyethylene at a high temperature under a high pressure.[1−3] This hexagonal phase plays an important role because chain-extended morphology is realized by annealing in the hexagonal phase. The structure of the hexagonal phase was investigated by differential thermal analysis (DTA),[1] optical microscopy,[4] X-ray diffraction,[5,6] Raman spectroscopy,[7] and ultrasonic measurements.[8] These experimental studies suggested that the high-pressure phase of polyethylene consists of statistically disordered conformations. Direct evidence of the existence of many gauche conformations was also brought by Raman spectroscopy.[7] Recent molecular dynamics simulations proposed the idea of the conformationally disordered (condis) phase for the hexagonal phase.[9−11] Though high-resolution solid-state ^{13}C NMR spectroscopy is also a powerful technique to elucidate the phase structure and molecular motion,[12−17] there is a difficulty in NMR measurements under such a high pressure (above 3.6 kbar).[1,18,19]

Some kinds of *n*-alkanes involve orthorhombic-to-hexagonal phase transition even at an atmospheric pressure before fusion with increasing temperature.[20−22] The molecular motion of the hexagonal (or rotator) phase of *n*-alkanes was studied by using solid-state ^{13}C NMR spectroscopy.[23−26] Unfortunately, however, the internal chains of hexagonal *n*-alkanes involve no gauche conformation,[20−22] and it is not appropriate to use them as model compounds for the hexagonal phase of polyethylene at a high temperature under a high pressure.

Recently, it has been found that the hexagonal phase also appears prior to melting in ultradrawn polyethylene fibers even at an atmospheric pressure under a constrained condition.[27,28] This type of hexagonal phase also includes gauche conformations.[29] In this work, we characterize the molecular motion in the hexagonal phase of polyethylene by using constrained ultradrawn polyethylene fibers. The results thus obtained are compared to the molecular motions in the hexagonal phase of *n*-alkanes[26] as well as in the orthorhombic phase of polyethylene at temperatures near the orthorhombic-to-hexagonal phase transition.

Experimental Section

Sample. In this study, ultradrawn polyethylene fibers Dyneema supplied by Toyobo Co. Ltd. were used without further purification, a weight-average molecular weight and a tensile modulus being 3×10^6 and 130 GPa, respectively.

DSC. DSC 2920 (TA Instruments) was operated at a heating rate of 1 °C/min. The temperature was calibrated with high-purity indium standards.

Solid-State ^{13}C NMR. High-resolution solid-state ^{13}C NMR measurements were performed on a Chemagnetics CMX-400 spectrometer operating under a static magnetic field of 9.4 T. The sample was packed into a 7.5 mm diameter zirconia rotor. Both ^1H and ^{13}C radio-frequency fields $\gamma B_1/2\pi$ were 62.5 kHz. The contact time for the cross-polarization (CP) process was 1.0 ms throughout this work. The magic angle spinning (MAS) rate was set to 3 kHz to avoid the overlapping of spinning sidebands on other resonance lines. ^{13}C chemical shifts were expressed as values relative to tetramethylsilane (Me_4Si) by using the CH_3 line at 17.36 ppm of hexamethylbenzene crystals as an external reference. ^{13}C spin−lattice relaxation times (T_{1C}) were measured by the CPT1 pulse sequence.[30]

CP/dipolar decoupling (CP/DD) ^{13}C NMR measurements were carried out for uniaxially oriented fibers without MAS by using a JEOL JNM-GSX200 spectrometer at a static magnetic field of 4.7 T. The orientation axis of fibers was set parallel or perpendicular to the static magnetic field B_0.

Sample Holders. Figure 1 shows the sample holders used in this work. Their materials were copper for DSC, Vespel for CP/MAS ^{13}C NMR, and Teflon for CP/DD ^{13}C NMR measurements. The polyethylene fibers were wound around the holders, and both ends of the fibers were tied tightly.

Results and Discussion

(a) DSC. Figure 2 shows DSC curves obtained for the constrained polyethylene fibers. On the heating process,

10.1021/ma990701k CCC: $18.00
Published on Web 08/05/1999

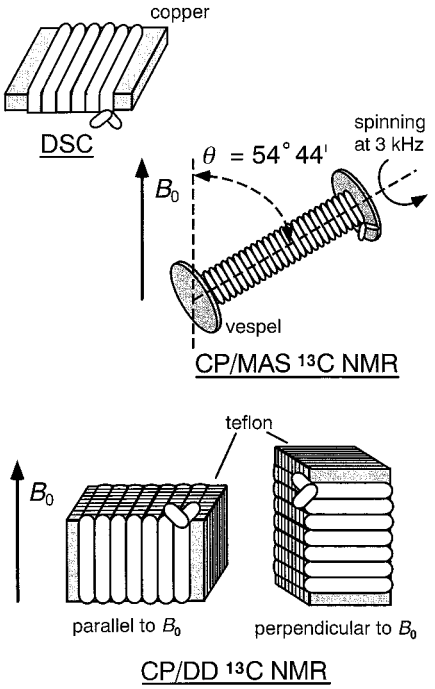

Figure 1. Sample holders used for the respective measurements.

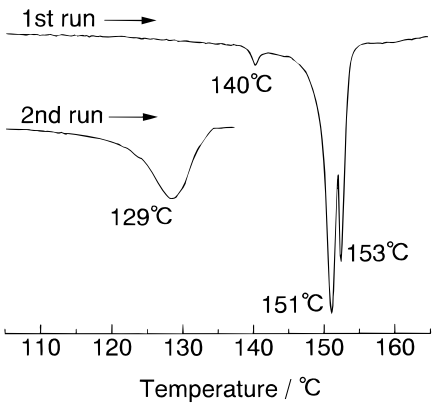

Figure 2. DSC curves for the constrained ultradrawn polyethylene fibers.

two endothermic peaks are observed at 151 and 153 °C, which correspond respectively to the orthorhombic-to-hexagonal phase transition and to melting of the hexagonal phase.[27,28] The small peak at 140 °C is ascribed to melting of the unconstrained parts of the polyethylene fibers. The curve of the constraint-free sample, measured as the second run, shows only one transition peak from the orthorhombic phase to the melt. These results are in good accord with the results previously reported for similar constrained ultradrawn polyethylene samples.[29]

(b) CP/MAS ^{13}C NMR Spectra. Figure 3 shows the CP/MAS ^{13}C NMR spectra of the constrained polyethylene fibers at 24−120 °C. The resonance line at 32.9 ppm is assigned to the orthorhombic crystalline component, whereas the line at 31 ppm that is more clearly observed at higher temperatures is ascribed to the noncrystalline component.[12] Two types of changes in line width are observed with increasing temperature: motional broadening of the crystalline component and motional narrowing for the noncrystalline component. These results indicate the onset of the molecular motion on the order of the dipolar decoupling field (about 10^5 Hz) for the crystalline component[31−33] and the further increase in frequency for much more enhanced motion ($>10^8$ Hz) for the noncrystalline component. The latter motion is conventionally recognized in different polyethylene samples. The former broadening has been found to be due to the 180° jump motion around the molecular chain axis.[34−36] This motion will further induce the chain diffusion along the chain axis as a result of the multistep forward and backward 180° jump motion.[34−39]

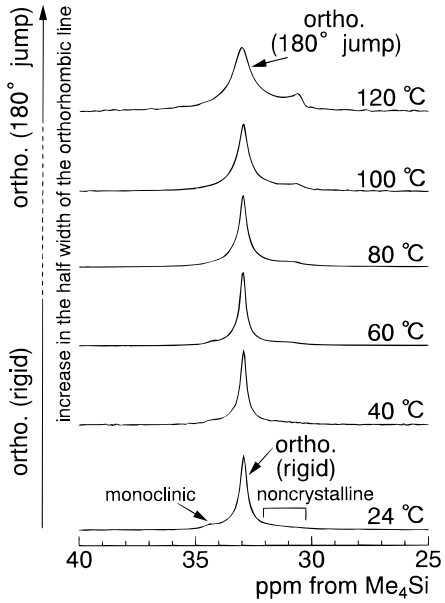

Figure 3. CP/MAS ^{13}C NMR spectra of the constrained ultradrawn polyethylene in the orthorhombic region.

The small resonance line at 34.7 ppm is ascribed to the monoclinic crystalline component[40] which is frequently produced for drawn polyethylene samples. The monoclinic-to-orthorhombic phase transition[41] occurs with the increase of temperature, and the monoclinic resonance line completely disappears above 80 °C.

CP/MAS ^{13}C NMR spectra at 120−152 °C for the constrained polyethylene fibers are shown in Figure 4. In accord with the appearance of an endothermic peak due to the orthorhombic-to-hexagonal phase transition at 145 °C in DSC, a new ^{13}C resonance line appears at 32.4 ppm above 145 °C. This line should be assigned to the CH_2 carbons in the hexagonal phase. Interestingly, this hexagonal line is observed significantly upfield compared to the orthorhombic resonance line at 32.9 ppm, whereas the corresponding hexagonal line appears downfield for *n*-alkanes.[23−25] Such an upfield shift in the hexagonal phase of polyethylene can be explained by the γ-gauche effect as a result of the transient introduction of gauche defects at random along the molecular chain and their rapid recovery transition to the original trans conformations.

On the basis of the chemical shifts, we calculate the amount of gauche conformations in the hexagonal phase of the constrained polyethylene fibers. In this calculation, the following three assumptions are made. First, the rapid transition between the trans and gauche conformations occurs independently at random in each crystalline C−C bond at a rate more than several tens of hertz. Second, the upfield shifts of the ^{13}C chemical shift values due to the γ-gauche and vicinal gauche effects are 5.0 and 2.5 ppm, respectively.[42] It should be noted here that the γ-gauche and vicinal gauche effects

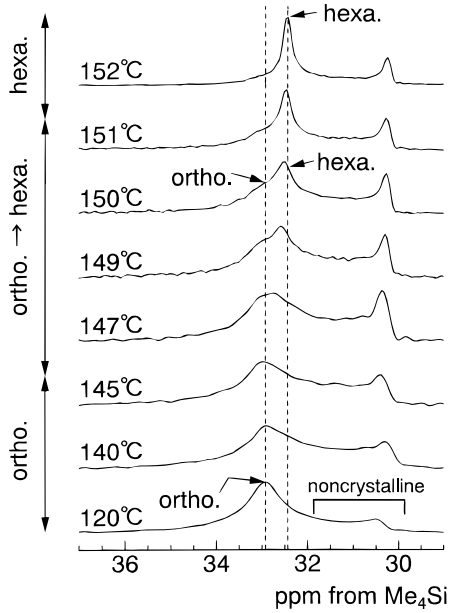

Figure 4. CP/MAS ^{13}C NMR spectra of the constrained ultradrawn polyethylene fibers in the orthorhombic-to-hexagonal phase transition region.

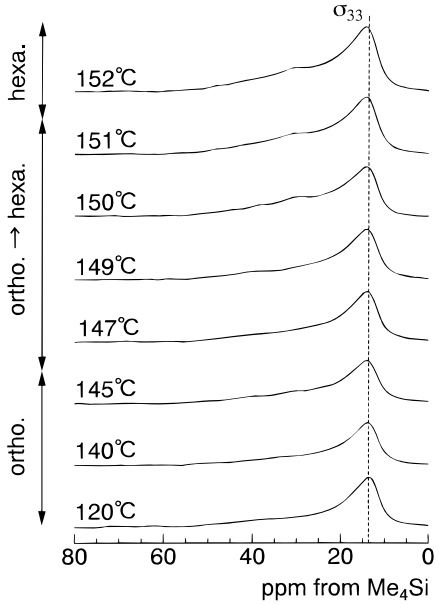

Figure 5. CP/DD ^{13}C NMR spectra of the constrained ultradrawn polyethylene fibers obtained by setting the orientation axis parallel to B_0.

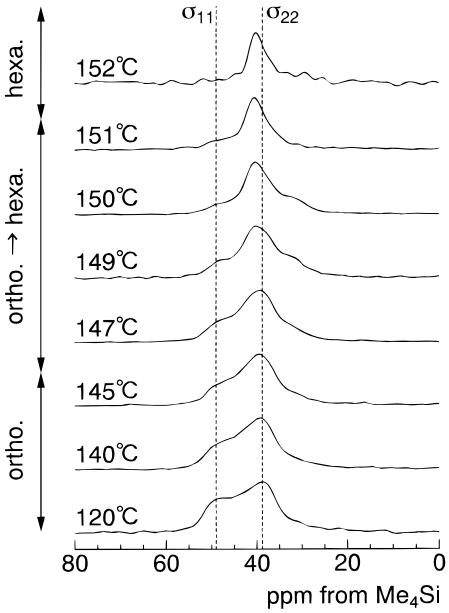

Figure 6. CP/DD ^{13}C NMR spectra of the constrained ultradrawn polyethylene fibers obtained by setting the orientation axis perpendicular to B_0.

do not depend on whether gauche conformations exist as isolated or not. Third, the downfield shift due to the difference in packing effect between the orthorhombic and hexagonal phases is assumed to be 0.5 ppm.[23−25] The following equation can be derived by using the mole fraction f_g of the gauche conformation:

$$-2(5.0 + 2.5)f_g + 0.5 = 32.4-32.9$$

According to this calculation, it is found that 7% gauche defects are included in the hexagonal phase for the constrained ultradrawn polyethylene fibers.

Recent molecular dynamics simulations revealed that ca. 10% gauche conformations are included in the conformationally disordered (condis) phase for long chain *n*-alkanes.[9−11] Separate Raman spectroscopic measurements found that more than 20% gauche conformations exist in the hexagonal phase for constrained ultradrawn polyethylene films.[29] However, most conformations are considered not to be simply defined trans and gauche conformations in the hexagonal phase; there must be considerable amounts of disordered trans and gauche conformations. Therefore, there may be some deviation in the estimation of gauche fractions depending on methodology.

(c) CP/DD ^{13}C NMR. Figure 5 shows CP/DD ^{13}C NMR spectra of the constrained polyethylene fibers obtained by setting the orientation axis of fibers parallel to B_0. The single resonance line appears at the most upfield principal value σ_{33} for the crystalline methylene carbons at each temperature. The σ_{33} axis is assigned to the direction parallel to the molecular chain axis in the orthorhombic polyethylene crystals.[43] No remarkable change is observed in the σ_{33} chemical shift even in the hexagonal phase, indicating that the overall molecular chain axis is not appreciably changed even if the rapid transition occurs between the trans and gauche conformations. This suggests that some kinks composed of the gauche−trans−gauche units may be produced at random along the molecular chain axis because such kinks do not alter the parallel orientation associated with the σ_{33} line for most of CH_2 carbons. Only two central CH_2 carbons in these kinks will give two resonance lines possibly at the downfield side compared to σ_{33} in the rigid state. In the present case, however, rapid exchange motion may induce averaging out between these small lines and the large σ_{33} line. This model may be supported by the detection of the minor downfield shift of the σ_{33} line in the hexagonal phase as is seen in Figure 5.

The CP/DD ^{13}C NMR spectra obtained by setting the orientation axis of the fibers perpendicular to B_0 are shown in Figure 6. At lower temperatures, two crystalline resonance lines appear at σ_{11} and σ_{22}, whose axes are ascribed to the directions parallel to the intramethylene H−H vector and to the H−C−H angle bisector, respectively.[43] Some contribution from the noncrystalline component should be superposed on the line at σ_{22}. As the temperature is increased through the ortho-

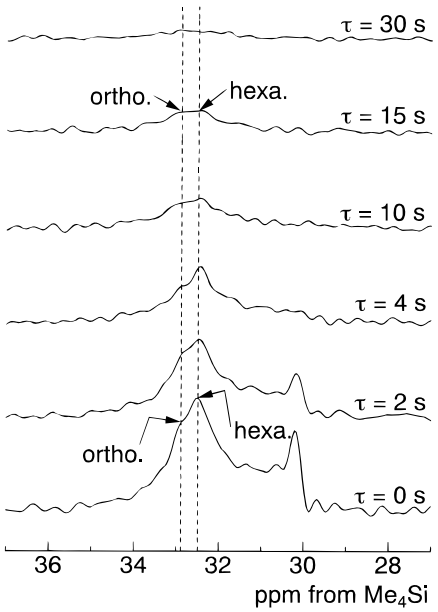

Figure 7. Partially relaxed MAS ^{13}C NMR spectra of the constrained ultradrawn polyethylene fibers at 150 °C, obtained by the CPT1 pulse sequence.

rhombic-to-hexagonal phase transition region, these two resonance lines merge to a single line. This fact implies that the overall jump rotation of some parts of each molecular chain will occur basically around the molecular chain axis in the hexagonal phase, resulting in the realization of the cylindrical symmetry of each molecular chain.[11] Moreover, this single line appears upfield compared to the average of the orthorhombic σ_{11} and σ_{22} values. Such an upfield shift may be induced by the γ-gauche effect due to the introduction of gauche defects and the rapid recovery transition to the trans conformations, in accord with the interpretation for the upfield shift of the isotropic chemical shift shown in Figure 4. It should be noted here that a recent quantum chemical calculation confirmed that the γ-gauche effect appears more effectively for the σ_{11} and σ_{22} components than for the σ_{33} component.[44]

(d) ^{13}C Spin−Lattice Relaxation Behavior. Figure 7 shows partially relaxed MAS ^{13}C NMR spectra of the constrained polyethylene fibers at 150 °C, obtained by the CPT1 pulse sequence.[30] As is clearly seen in the figure, the ^{13}C spin−lattice relaxation behavior is almost the same for the orthorhombic and hexagonal phases. This means that the spectral densities of molecular motions near 10^8 Hz associated with the ^{13}C spin−lattice relaxation are similar in the two phases.

In Figure 8, T_{1C} values are plotted against temperature for the crystalline component of the constrained polyethylene fibers, which are obtained by setting the orientation axis of the fibers parallel or perpendicular to B_0. The T_{1C} values are as long as about 2000 s at 24 °C under both setting conditions. With the increase of temperature, the T_{1C} value abruptly decreases in the orthorhombic region as a result of the enhanced local motion probably induced by the onset of the 180° jump motion. At temperatures over the orthorhombic-to-hexagonal phase transition, the T_{1C} value further decreases possibly due to the high-frequency local fluctuation associated with the random introduction of gauche defects along each molecular chain. Figure 8 also reveals that the spectral densities near 10^8 Hz of such

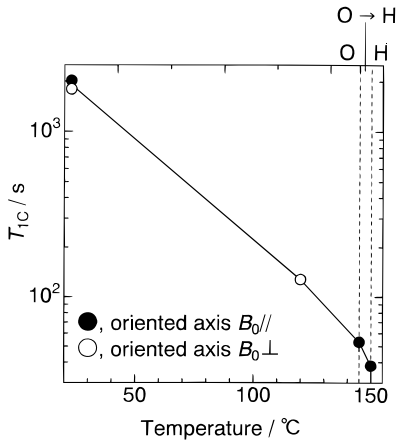

Figure 8. T_{1C} vs temperature for the crystalline component of the constrained ultradrawn polyethylene fibers by setting the orientation axis of fibers parallel or perpendicular to B_0. "O" and "H" denote the orthorhombic and hexagonal phases, respectively.

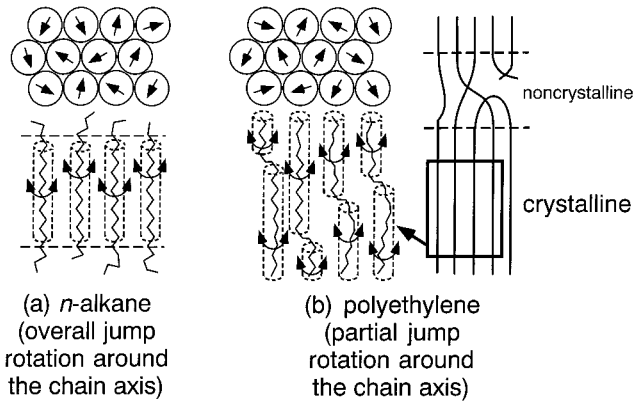

Figure 9. Illustrated molecular motions in the hexagonal phase for *n*-alkane and polyethylene.

local motions are not significantly different in the orthorhombic and hexagonal phases.

This situation is similar to the temperature dependence of the T_{1C} values for *n*-$C_{27}H_{56}$ crystals.[26] Solid *n*-$C_{27}H_{56}$ involves orthorhombic-to-monoclinic and monoclinic-to-hexagonal phase transitions at 53 and 60 °C, respectively. However, while the T_{1C} values were remarkably decreased with the increase of temperature from 0 to 60 °C, there was no sharp break even at the phase transition temperatures, just as is observed here in the phase transition region.

(e) Schematic Diagrams for the Hexagonal Phase. Figure 9 shows the illustrated structures of the hexagonal phases for *n*-alkanes[26] and the constrained ultradrawn polyethylene fibers. The lamellar thicknesses of *n*-alkane crystals are of the order of 2−5 nm. In the hexagonal phase of these crystals, each molecular chain is allowed to undergo the overall jump rotation with random jump angles around the molecular chain axis keeping the planar zigzag conformation.[20−22,26] Such motion will be preferable to fulfill the cylindrical symmetry of the molecular chain in the hexagonal phase. In contrast, the lamellar thickness of the ultradrawn polyethylene fibers is as large as about 40 nm.[45] Moreover, both ends of the crystalline chains should be connected to the noncrystalline chains. Under these circumstances, it may be difficult to simply induce the random jump rotation of the whole crystalline chain around the molecular chain axis unlike *n*-alkanes.

Accordingly, several percent gauche defects must be introduced at random along the respective chains to allow independent jump rotations around the chain axis for the almost planar zigzag CH_2 sequences between the gauche defects in the polyethylene fibers, as shown in Figure 9b. When kink defects composed of gauche−trans−gauche units are introduced, the average stem length of the partial jump rotation will be 3−4 nm because 4−3 kinks exist per 100 methylenes.

It is well-known that the dynamic mechanical analysis of polyethylene prior to melting reveals at least three mechanical relaxations, designated as α, β, and γ in the order of decreasing temperature.[46] The mechanical α relaxation consists of at least three subrelaxations, namely α_1, α_2, and α_3 in the order of increasing temperature.[47] The α_1 relaxation arises from the interlamellar slip[48] or the deformation of intermosaic regions within the crystalline lamellae.[49] The α_2 relaxation is believed to originate from the thermal oscillation of intracrystalline polymer chains,[47−49] including twisting motion about the *c*-axis as well as translational motion along the *c*-axis.[50,51] The reality of the α_3 relaxation is suggested to be associated with the transition from the orthorhombic phase to the hexagonal phase.[52,53] The α relaxation temperature for polyethylenes is somewhat diffuse, ranging from 30 to 120 °C.[46,50,51] When a polyethylene sample is measured by solid-state ^{13}C NMR spectroscopy near the α relaxation temperature, the spectra mainly reflect the α_2 and α_3 relaxations. In the constrained polyethylene fibers, the 180° jump motion shown in Figure 3 is considered to be correlated with the α_2 relaxation. The orthorhombic-to-hexagonal phase transition shown in Figures 4−6 is considered to be the origin of the α_3 relaxation.

Conclusions

The orthorhombic-to-hexagonal phase transition for constrained polyethylene fibers has been investigated by solid-state ^{13}C NMR spectroscopy, and the following conclusions have been obtained.

(1) In the CP/MAS ^{13}C NMR spectra, the CH_2 resonance line in the hexagonal phase is observed upfield compared to the orthorhombic resonance line. The calculation of the ^{13}C chemical shift for this line has revealed that 7% gauche defects are included in the hexagonal phase.

(2) In the CP/DD ^{13}C NMR spectra obtained by setting the fiber axis perpendicular to B_0, two resonance lines appearing at σ_{11} and σ_{22} in the orthorhombic phase are found to merge to a single line in the hexagonal phase. Moreover, the chemical shift of the single line is also somewhat lower compared to the average of σ_{11} and σ_{22}. In contrast, no remarkable change is observed for the resonance line at σ_{33} in the two phases when the CP/DD ^{13}C NMR spectra are measured by setting the fiber axis parallel to B_0. On the basis of these experimental results, the following structure model has been proposed for the molecular motion in the hexagonal phase for the constrained ultradrawn polyethylene fibers: Several percent gauche defects are introduced probably as kinks composed of the gauche−trans−gauche units at random along the respective molecular chains. Concomitantly, jump rotations with random jump angles are allowed to occur around the molecular chain axis for almost planar zigzag CH_2 sequences between these gauche defects. Such partial jump rotations between the gauche defects may inevitably be induced in the hexagonal phase for thicker lamellar crystals in the constrained ultradrawn polyethylene fibers.

(3) The CP/MAS ^{13}C NMR spectra are found to broaden markedly with increasing temperature below the orthorhombic-to-hexagonal phase transition temperature. This fact indicates that the 180° jump motion occurs with a frequency of about 10^5 Hz in the orthorhombic phase at this temperature range, and the chain diffusion along each molecular chain will probably be induced as a result of the multistep forward and backward 180° jump rotations.

Acknowledgment. The authors thank Toyobo Co. Ltd. for kindly supplying the ultradrawn polyethylene fibers (Dyneema).

References and Notes

(1) Bassett, D. C.; Khalifa, B. A.; Turner, B. *Nature* (*Phys. Sci.*) **1972**, *239*, 106; **1972**, *240*, 146.
(2) Wunderlich, B.; Grebowicz, J. *Liquid Crystal Polymers II/III*; Springer-Verlag: Berlin, 1984; pp 40−49.
(3) Bassett, D. C. *Developments in Crystalline Polymers* 2; Applied Science: London, 1988; pp 67−103.
(4) Yasuniwa, M.; Takemura, T. *Polym. J.* **1974**, *15*, 661.
(5) Bassett, D. C.; Block, S.; Piermarini, G. J. *J. Appl. Phys.* **1974**, *45*, 4146.
(6) Yasuniwa, M.; Enoshita, R.; Takemura, T. *Jpn. J. Appl. Phys.* **1976**, *15*, 1421.
(7) Yamamoto, T. *J. Macromol. Sci. Phys.* **1979**, *B16*, 487.
(8) Nagata, K.; Tagashira, K.; Taki, S.; Takemura, T. *Jpn. J. Appl. Phys.* **1981**, *19*, 985.
(9) Sumpter, B. G.; Noid, D. W.; Wunderlich, B. *J. Chem. Phys.* **1990**, *93*, 6875.
(10) Noid, D. W.; Sumpter, B. G. *Macromolecules* **1990**, *23*, 664.
(11) Liang, G. L.; Noid, D. W.; Sumpter, B. G.; Wunderlich, B. *J. Polym. Sci., Polym. Phys. Ed.* **1993**, *31*, 1909.
(12) Kitamaru, R.; Horii, F.; Murayama, K. *Macromolecules* **1986**, *19*, 636.
(13) Kimura, T.; Neki, K.; Tamura, N.; Horii, F.; Nakagawa, M.; Odani, H. *Polymer* **1992**, *33*, 4140.
(14) Kitamaru, R.; Horii, F.; Zhu, Q.; Bassett, D. C.; Olley, R. H. *Polymer* **1994**, *35*, 1171.
(15) Kuwabara, K.; Kaji, H.; Horii, F.; Bassett, D. C.; Olley, R. H. *Macromolecules* **1997**, *30*, 7516.
(16) Horii, F.; Kaji, H.; Ishida, H.; Kuwabara, K.; Masuda, K.; Tai, T. *J. Mol. Struct.* **1998**, *441*, 303.
(17) Nakaoki, T.; Ohira, Y.; Hayashi, H.; Horii, F. *Macromolecules* **1998**, *31*, 2705.
(18) Rastogi, S.; Hikosaka, M.; Kawabata, H.; Keller, A. *Macromolecules* **1991**, *24*, 6384.
(19) Rastogi, S.; Kurelec, L.; Lemstra, P. J. *Macromolecules* **1998**, *31*, 5022.
(20) Strobl, G.; Ewen, B.; Fischer, E. W.; Piesczek, W. *J. Chem. Phys.* **1974**, *61*, 5257.
(21) Ewen, B.; Fischer, E. W.; Piesczek, W.; Strobl, G. *J. Chem. Phys.* **1974**, *61*, 5265.
(22) Ewen, B.; Strobl, G. R.; Richter, D. *J. Chem. Soc., Faraday Discuss.* **1980**, *69*, 19.
(23) Möller, M.; Cantow, H.-J.; Drotloff, H.; Emeis, D.; Lee, K.-S.; Wegner, G. *Macromol. Chem.* **1986**, *187*, 1237.
(24) VanderHart, D. L. *J. Magn. Reson.* **1981**, *44*, 117.
(25) Ishikawa, S.; Kurosu, H.; Ando, I. *J. Mol. Struct.* **1991**, *248*, 361.
(26) Kitamaru, R.; Horii, F.; Nakagawa, M.; Takamizawa, K.; Urabe, Y.; Ogawa, Y. *J. Mol. Struct.* **1995**, *355*, 95.
(27) Pennings, A. J.; Zwijnenburg, A. *J. Polym. Sci., Polym. Phys. Ed.* **1979**, *17*, 1011.
(28) van Aerle, N. A. J. M.; Lemstra, P. J. *Polym. J.* **1988**, *20*, 131.
(29) Tashiro, K.; Sasaki, S.; Kobayashi, M. *Macromolecules* **1996**, *29*, 7460.
(30) Torchia, D. A. *J. Magn. Reson.* **1978**, *30*, 613.
(31) Suwelack, D.; Rothwell, W. P.; Waugh, J. S. *J. Chem. Phys.* **1980**, *73*, 2559.
(32) Rothwell, W. P.; Waugh, J. S. *J. Chem. Phys.* **1981**, *74*, 2721.
(33) Takegoshi, K.; Hikichi, K. *J. Chem. Phys.* **1991**, *94*, 3200.
(34) Kuwabara, K.; Kaji, H.; Horii, F.; Bassett, D. C.; Olley, R. H. *Polym. Prep. Jpn.* **1996**, *45*, 799.

(35) Hillebrand, L.; Schmidt, A.; Bolz, A.; Hess, M.; Veeman, W. *Macromolecules* **1998**, *31*, 5010.
(36) Hu, W.-G.; Boeffel, C.; Schmidt-Rohr, K. *Macromolecules* **1999**, *32*, 1611, 1714.
(37) Schmidt-Rohr, K.; Spiess, H. W. *Macromolecules* **1991**, *24*, 5288.
(38) Robertson, M. B.; Ward, I. M.; Klein, K. G.; Packer, K. J. *Macromolecules* **1997**, *30*, 6893.
(39) Klein, P. G.; Robertson, M. B.; Driver, M. A. N.; Ward, I. M.; Packer, K. J. *Polym. Int.* **1998**, *47*, 76.
(40) VanderHart, D. L. *Polymer* **1984**, *25*, 830.
(41) Seto, T.; Hara, T.; Tanaka, K. *Jpn. J. Appl. Phys.* **1968**, *7*, 31.
(42) Möller, M.; Gronski, W.; Cantow, H.-J.; Höcker, H. *J. Am. Chem. Soc.* **1984**, *106*, 5093.
(43) VanderHart, D. L. *J. Chem. Phys.* **1976**, *64*, 830.
(44) Kurosu, H., private communication.
(45) Smith, P.; Lemstra, P. J.; Pijpers, J. P. L.; Kiel, A. M. *Colloid Polym. Sci.* **1981**, *259*, 1070.
(46) McCrum, N. G.; Read, B. E.; Williams, G. *Anelastic and Dielectric Effects in Polymer Solids*; Wiley: New York, 1967.
(47) Nakayasu, H.; Markovitz, H.; Plazek, D. *J. Trans. Soc. Rehol.* **1961**, *5*, 261.
(48) Cembrola, R. J.; Stein, R. S. *J. Polym. Sci., Polym. Phys. Ed.* **1980**, *18*, 1065.
(49) Takayanagi, M.; Matsuo, T. *J. Macromol. Sci., Phys.* **1967**, *B1*, 407.
(50) Boyd, R. H. *Polymer* **1985**, *26*, 323.
(51) Boyd, R. H. *Polymer* **1985**, *26*, 1123.
(52) Matsuo, M.; Sawatari, C.; Ohhata, T. *Macromolecules* **1988**, *21*, 1317.
(53) Ohta, Y.; Yasuda, H. *J. Polym. Sci., Polym. Phys. Ed.* **1994**, *32*, 2241.

MA990701K